Mon. Not. R. Astron. Soc. **331,** 245–258 (2002)

Mass segregation in young compact star clusters in the Large Magellanic Cloud – II. Mass functions

R. de Grijs,[1★] G. F. Gilmore,[1] R. A. Johnson[1,2] and A. D. Mackey[1]
[1]*Institute of Astronomy, University of Cambridge, Madingley Road, Cambridge CB3 0HA*
[2]*European Southern Observatory, Casilla 19001, Santiago 19, Chile*

Accepted 2001 November 19. Received 2001 November 16; in original form 2001 November 5

ABSTRACT

We review the complications involved in the conversion of stellar luminosities into masses and apply a range of mass-to-luminosity relations to our *Hubble Space Telescope* observations of the young Large Magellanic Cloud (LMC) star clusters NGC 1805 and 1818.

Both the radial dependence of the mass function (MF) and the dependence of the cluster core radii on mass indicate clear mass segregation in both clusters at radii of $r \lesssim 20-30$ arcsec, for masses in excess of $\sim 1.6-2.5\,\mathrm{M}_\odot$. This result does not depend on the mass range used to fit the slopes or the metallicity assumed. It is clear that the cluster MFs, at any radius, are not simple power laws.

The global and the annular MFs near the core radii appear to be characterized by similar slopes in the mass range ($-0.15 \leqslant \log m/\mathrm{M}_\odot \leqslant 0.85$), and the MFs beyond $r \gtrsim 30$ arcsec have significantly steeper slopes.

We estimate that while the NGC 1818 cluster core is between ~ 5 and ~ 30 crossing times old, the core of NGC 1805 is likely to be $\lesssim 3-4$ crossing times old. However, since strong mass segregation is observed out to $\sim 6R_{\rm core}$ and $\sim 3R_{\rm core}$ in NGC 1805 and 1818, respectively, it is most likely that significant primordial mass segregation was present in both clusters, particularly in NGC 1805.

Key words: stars: luminosity function, mass function – Magellanic Clouds – galaxies: star clusters.

1 PRIMORDIAL VERSUS DYNAMICAL MASS SEGREGATION

The effects of mass segregation in star clusters, with the more massive stars being more centrally concentrated than the lower-mass stars, clearly complicates the interpretation of an observed luminosity function (LF) at a given position within a star cluster in terms of its initial mass function (IMF). Without reliable corrections for the effects of mass segregation, and hence for the structure and dynamical evolution of the cluster, it is impossible to obtain a realistic global cluster LF.

1.1 Dynamical evolution in star cluster cores

Dynamical evolution in dense stellar systems, such as Galactic globular clusters (GCs) and rich Large Magellanic Cloud (LMC) star clusters, drives the systems towards energy equipartition, in which the lower-mass stars will attain higher velocities and therefore occupy larger orbits.

★E-mail: grijs@ast.cam.ac.uk

Consequently, the high-mass stars will gradually sink towards the bottom of the cluster potential, i.e. the cluster centre (cf. Spitzer & Hart 1971), with the highest-mass stars and those closest to the cluster centre sinking the fastest, although this process is not negligible even at the edge of the cluster (e.g. Chernoff & Weinberg 1990; Hunter et al. 1995). This leads to a more centrally concentrated high-mass component compared with the lower-mass stellar population, and thus to dynamical mass segregation.

The time-scale for the onset of significant dynamical mass segregation is comparable to the dynamical relaxation time of the cluster (Spitzer & Shull 1975; Inagaki & Saslaw 1985; Bonnell & Davies 1998; Elson et al. 1998). The characteristic time-scale of a cluster may be taken to be its half-mass (or median) relaxation time, i.e. the relaxation time at the mean density for the inner half of the cluster mass for cluster stars with stellar velocity dispersions characteristic for the cluster as a whole (Spitzer & Hart 1971; Lightman & Shapiro 1978; Meylan 1987; Malumuth & Heap 1994; Brandl et al. 1996), and can be written as (Meylan 1987)

$$t_{\rm r,h} = (8.92\times10^5)\frac{M_{\rm tot}^{1/2}}{\langle m\rangle}\frac{R_{\rm h}^{3/2}}{\log(0.4M_{\rm tot}/\langle m\rangle)}\,\mathrm{yr}, \quad (1)$$

where $R_{\rm h}$ is the half-mass (median) radius (in pc), $M_{\rm tot}$ is the total cluster mass and $\langle m \rangle$ is the typical mass of a cluster star (both masses in $\mathrm{M}_{\odot}$).

Although the half-mass relaxation time characterizes the dynamical evolution of a cluster as a whole, significant differences are expected locally within the cluster. From equation (1) it follows immediately that the relaxation time-scale will be shorter for higher-mass stars (greater $\langle m \rangle$) than for their lower-mass companions; numerical simulations of realistic clusters confirm this picture (e.g. Aarseth & Heggie 1998, see also Hunter et al. 1995; Kontizas et al. 1998). From this argument it follows that dynamical mass segregation will also be most rapid where the local relaxation time is shortest, i.e. near the cluster centre (cf. Fischer et al. 1998; Hillenbrand & Hartmann 1998). The relaxation time in the core can be written as (Meylan 1987)

$$t_{\rm r,0} = (1.55 \times 10^7) \frac{v_{\rm s} R_{\rm core}^2}{\langle m_0 \rangle \log(0.5 M_{\rm tot}/\langle m \rangle)} \,\mathrm{yr}, \qquad (2)$$

where $R_{\rm core}$ is the cluster core radius (in pc), $v_{\rm s}$ ($\mathrm{km\,s^{-1}}$) is the velocity scale and $\langle m_0 \rangle$ is the mean mass (in $\mathrm{M}_{\odot}$) of all particles in thermal equilibrium in the central parts.

Thus, significant mass segregation among the most massive stars in the cluster core occurs on the local, central relaxation time-scale (comparable to just a few crossing times, cf. Bonnell & Davies 1998), whereas a time-scale $\propto t_{\rm r,h}$ is required to affect a large fraction of the cluster mass.

It should be borne in mind, however, that even the concept of a 'local relaxation time' is only a general approximation, as dynamical evolution is a continuing process. The time-scale for a cluster to lose all traces of its initial conditions also depends on the smoothness of its gravitational potential, i.e. the number of stars (Bonnell & Davies 1998: larger clusters are inherently smoother, and therefore mass segregation is slower than in smaller clusters with a grainier mass distribution), the degree of equipartition reached (e.g. Hunter et al. 1995: full global, or even local, equipartition is never reached in a realistic star cluster, not even among the most massive species), and the slope of the MF (e.g. Lightman & Shapiro 1978; Inagaki & Saslaw 1985; Pryor, Smith & McClure 1986; Sosin 1997: flatter mass spectra will speed up the dynamical evolution, whereas steep mass spectra will tend to a higher degree of equipartition), among others.

In addition, as the more massive stars move inwards towards the cluster centre, their dynamical evolution will speed up, and hence the dynamical relaxation time-scale for a specific massive species is hard to define properly. This process will be accelerated if there is no (full) equipartition (cf. Inagaki & Saslaw 1985), thus producing high-density cores very rapidly, where stellar encounters occur very frequently and binary formation is thought to be very effective (cf. Inagaki & Saslaw 1985; Elson, Hut & Inagaki 1987b). In fact, the presence of binary stars may accelerate the mass segregation significantly, since two-body encounters between binaries and between binaries and single stars are very efficient (e.g. Nemec & Harris 1987; De Marchi & Paresce 1996; Bonnell & Davies 1998; Elson et al. 1998). This process will act on similar (or slightly shorter) time-scales to the conventional dynamical mass segregation (cf. Nemec & Harris 1987; Bonnell & Davies 1998; Elson et al. 1998). In summary, the time-scale for dynamical relaxation is a strong function of position within a cluster, and varies with its age.

1.2 Primordial mass segregation

Although a cluster will have lost all traces of its initial conditions on time-scales longer than its characteristic relaxation time, on shorter time-scales the observed stellar density distribution is likely to be the result of dynamical relaxation and of the way that star formation has taken place. The process is, in fact, more complicated, as the high-mass stars evolve on the same time-scale as the lower-mass stars (cf. Aarseth 1999). In order to understand the process of mass segregation in a cluster in detail, we have to get an idea of the amount of 'primordial' mass segregation in the cluster.

The nature and degree of primordial mass segregation is presumably determined by the properties of interactions of protostellar material during the star-forming episode in a cluster. In the classic picture of star formation (Shu, Adams & Lizano 1987), interactions are unimportant and mass segregation does not occur. However, Fischer et al. (1998) conclude that their observations of NGC 2157 seem to indicate the picture in which encounters at the early stages in the evolution enhance mass accretion of the cluster caused by the merging of protostellar clumps until the mass of these clumps exceeds the initial mass of a star to be formed. More massive stars are subject to more mergers and hence accrete even more mass (cf. Larson 1991; Bonnell et al. 2001a,b and references therein), and therefore dissipate more kinetic energy. In addition, they tend to form near the cluster centre, in the highest-density region, where the encounter rate is highest (cf. Larson 1991; Bonnell et al. 1997, 2001a,b; Bonnell, Bate & Zinnecker 1998; Bonnell & Davies 1998). This will lead to an observed position-dependent MF containing more low-mass stars at larger radii compared with the MF in the cluster centre (although low-mass stars are still present at small radii). This scenario is fully consistent with the idea that more massive stars tend to form in clumps and lower-mass stars form throughout the cluster (Hunter et al. 1995; Brandl et al. 1996, and references therein).

Although it has been claimed that the observed mass segregation in R136, the central cluster in the large star-forming complex 30 Doradus in the LMC, is probably at least partially primordial (e.g. Malumuth & Heap 1994; Brandl et al. 1996), its age of $\simeq$3–4 Myr is sufficiently long for at least some dynamical mass segregation, in particular of the high-mass stars in the core ($r \lesssim 0.5$ pc), to have taken place (cf. Malumuth & Heap 1994; Hunter et al. 1995; Brandl et al. 1996). On the other hand, the presence of the high-mass Trapezium stars in the centre of the very young Orion Nebula Cluster (ONC; $\lesssim$1 Myr, equivalent to $\simeq$3–5 crossing times; Bonnell & Davies 1998) is probably to be largely caused by mass segregation at birth (Bonnell & Davies 1998, based on numerical simulations; Hillenbrand & Hartmann 1998, based on the appearance of the cluster as non-dynamically relaxed, and references therein). Bonnell & Davies (1998) show convincingly that the massive stars in the core of the ONC most probably originated within the inner 10–20 per cent of the cluster.

Hillenbrand & Hartmann (1998) argue that the young embedded clusters NGC 2024 and Monoceros R2 also show evidence for primordial mass segregation, since the outer regions of these clusters (and of the ONC as well) are not even one crossing time old.

2 THE DATA

As part of *Hubble Space Telescope* (*HST*) programme GO-7307, we obtained deep WFPC2 *V*- and *I*-band imaging of seven rich, compact star clusters in the LMC, covering a large age range. In de Grijs et al. (2001, hereafter Paper I) we presented the observational data for the two youngest clusters in our sample, NGC 1805 and 1818, and discussed the dependence of the LFs on radius within

each cluster. We found clear evidence for luminosity segregation within the inner ∼30 arcsec for both clusters, in the sense that the inner annular LFs showed a relative overabundance of bright stars with respect to the less luminous stellar population compared with the outer annular LFs.

In this paper, we will extend our analysis to the associated MFs and discuss the implications of our results in terms of the IMF and the star formation process. In Section 4 we will derive the MF slopes for both clusters, using a number of mass-to-luminosity (ML) conversions discussed in Section 3. We will take care to only include main-sequence stars belonging to the clusters in our final MFs; to do so, we will exclude the field LMC red giant branch stars from the colour–magnitude diagrams (CMDs), with colours $(V-I) \geq 0.67$ if they are brighter than $V = 22$ mag (see the CMDs in Johnson et al. 2001 for comparison). In fact, as can be seen from these CMDs, the true structure of the Hertzsprung–Russell (HR) diagram above the main-sequence turn-off is very complex. Stellar populations of different masses overlap in colour–magnitude space, so that an unambiguous mass determination from isochrone fits, for the handful to the few dozen stars populating these areas in each cluster, is highly model dependent (cf. fig. 11 in Johnson et al. 2001). In a differential analysis such as presented in this paper, the uncertainties involved in their mass determinations are too large and systematic (i.e. model dependent), so that we cannot include these stars in our analysis.

Table 1 of Paper I contains the fundamental parameters for our two young sample clusters. For the analysis in this paper, however, we need to justify our choice for the adopted metallicity, age and cluster mass in more detail.

(i) *Cluster metallicities*. For NGC 1805, metallicity determinations are scarce. Johnson et al. (2001) obtained an estimate of near solar metallicity, from fits to *HST* CMDs. The only other metallicity estimate available for NGC 1805, [Fe/H] ~ -0.30 (Meliani, Barbuy & Richtler 1994) is based on the average metallicity of the young LMC population and is therefore less certain.

Abundance estimates for NGC 1818, on the other hand, are readily available, but exhibit a significant range. The most recent determination by Johnson et al. (2001), based on *HST* CMD fits, similarly suggests near-solar abundance, [Fe/H] ≈ 0.0. Metallicity determinations based on stellar spectroscopy range from roughly [Fe/H] ~ -0.8 (Meliani et al. 1994; Will, Bomans & de Boer 1995; Oliva & Origlia 1998) to [Fe/H] ~ -0.4 (Jasniewicz & Thévenin 1994; Bonatto, Bica & Alloin 1995; see also Johnson et al. 2001).

For the purposes of the present paper, we will consider the cases of [Fe/H] $= 0.0$ and [Fe/H] $= -0.5$ for both clusters.

(ii) *Age estimates*. Various age estimates exist for both clusters, which are all roughly consistent with each other, although they are based on independent diagnostics. The age range for NGC 1805 is approximately bracketed by $\log t(\mathrm{yr}) = 6.95$–$7.00$ (cf. Bica, Alloin & Santos 1990; Barbaro & Olivi 1991; Santos et al. 1995; Cassatella et al. 1996) and $\log t(\mathrm{yr}) = 7.6$–$7.7$ (cf. Barbaro & Olivi 1991), with the most recent determinations favouring younger ages. We will therefore adopt an age for NGC 1805 of $\log t(\mathrm{yr}) = 7.0^{+0.3}_{-0.1}$.

Numerous age estimates are available for NGC 1818, on average indicating a slightly older age for this cluster than for NGC 1805. Most estimates bracket the age range between $t \sim 15$ Myr (Bica et al. 1990; Bonatto et al. 1995; Santos et al. 1995; Cassatella et al. 1996) and $t \gtrsim 65$ Myr (cf. Barbaro & Olivi 1991), with the most recent estimates, based on *HST* CMD fits, favouring an age of $t \simeq 20$–30 Myr (e.g. Cassatella et al. 1996; Grebel et al. 1997; Hunter et al. 1997; van Bever & Vanbeveren 1997; Fabregat & Torrejón 2000). We will therefore adopt an age of $t \simeq 25$ Myr for NGC 1818, or $\log t(\mathrm{yr}) = 7.4^{+0.3}_{-0.1}$.

(iii) *Cluster masses*. To obtain mass estimates for both clusters, we first obtained the total *V*-band luminosity for each cluster based on fits to the surface brightness profiles of our longest CEN exposures, in order to retain a sufficiently high signal-to-noise ratio even for the fainter underlying stellar component. We subsequently corrected these estimates of $L_{V,\mathrm{tot}}$ for the presence of a large number of saturated stars in the long CEN exposures (i.e. the observations where we located the cluster centre in the WFPC2/PC chip) by comparison with the short CEN exposures. Although even in the short CEN exposures there are some saturated stars (cf. Section 3.3 in Paper I), their number is small (12 in NGC 1805 and 18 in NGC 1818), so that we can obtain firm lower limits of $\log L_{V,\mathrm{tot}}(L_{V,\odot}) = 4.847$ and 5.388 for NGC 1805 and 1818, respectively.

Models of single-burst simple stellar populations (e.g. Bruzual & Charlot 1996), which are fairly good approximations of coeval star clusters, predict mass-to-light (M/L) ratios as a function of age, which we can use to obtain photometric mass estimates for our clusters. This leads to mass estimates of $M_{\mathrm{tot}} = 2.8^{+3.0}_{-0.8} \times 10^3\,\mathrm{M}_\odot$ ($\log M_{\mathrm{tot}}/\mathrm{M}_\odot = 3.45^{+0.31}_{-0.15}$) for NGC 1805 and $M_{\mathrm{tot}} = 2.3^{+1.1}_{-0.3} \times 10^4\,\mathrm{M}_\odot$, or $\log M_{\mathrm{tot}}/\mathrm{M}_\odot = 4.35^{+0.18}_{-0.05}$ for NGC 1818.

Our mass estimate for NGC 1805 is low compared with the only other available mass, $M_{\mathrm{tot}} = 6 \times 10^3\,\mathrm{M}_\odot$ (Johnson et al. 2001), although their mass estimate, based on earlier simple stellar population models, is close to the upper mass allowed by our 1σ uncertainty.

For NGC 1818, our mass estimate is entirely within the probable range derived by Elson, Fall & Freeman (1987a), i.e. $4.1 \leq \log M_{\mathrm{tot}}/\mathrm{M}_\odot \leq 5.7$, depending on the M/L ratio, and the estimate of Hunter et al. (1997) of $M_{\mathrm{tot}} = 3 \times 10^4\,\mathrm{M}_\odot$ falls comfortably within our 1σ uncertainty. The determination by Chrysovergis et al. (1989) of $\log M_{\mathrm{tot}}/\mathrm{M}_\odot = 4.69$ is outside our 1σ error bar; we speculate that the difference between our two estimates is caused by a combination of the single-mass isotropic King cluster model used by them versus our photometric mass determination, and a different treatment of the background stellar contribution.

3 CONVERTING LUMINOSITY TO MASS FUNCTIONS

The conversion of an observational LF (which we determined for NGC 1805 and 1818 in Paper I), in a given passband i, $\phi(M_i)$, to its associated MF, $\xi(m)$, is not as straightforward as is often assumed. The differential present-day stellar LF, $\mathrm{d}N/\mathrm{d}\phi(M_i)$, i.e. the number of stars in the absolute-magnitude interval $[M_i, M_i + \mathrm{d}M_i]$, and the differential present-day MF, $\mathrm{d}N/\mathrm{d}\xi(m)$, i.e. the mass in the corresponding mass interval $[m, m + \mathrm{d}m]$, are related through $\mathrm{d}N = -\phi(M_i)\,\mathrm{d}M_i = \xi(m)\,\mathrm{d}m$ (Kroupa 2000), and therefore

$$\phi(M_i) = -\xi(m)\frac{\mathrm{d}m}{\mathrm{d}M_i}. \qquad (3)$$

Thus, in order to convert an observational LF into a reliable MF, one needs to have accurate knowledge of the appropriate ML – or mass–absolute-magnitude – relation, $\mathrm{d}m/\mathrm{d}M_i$. Empirical ML relations are hard to come by, and so far have only been obtained for solar-metallicity stars (e.g. Popper 1980; Andersen 1991;

Henry & McCarthy 1993, hereafter HM93; Kroupa, Tout & Gilmore 1993, hereafter KTG93). The ML relation is, however, a strong function of the stellar metallicity, and one needs to include corrections for hidden companion stars to avoid introducing a systematic bias in the derived MF (e.g. KTG93; Kroupa 2000). For the conversion of the present-day MF to the IMF, one needs additional corrections for stellar evolution on and off the main sequence, including corrections for age, mass loss, spread in metallicity and evolution of rotational angular momentum or spin (cf. Scalo 1986; Kroupa 2000). Although the ML relation is relatively well-established for stars more massive than $\sim 0.8\,\mathrm{M}_\odot$, our rather limited understanding of the lower-mass, more metal-poor stars, especially of the boundary conditions between the stellar interior and their atmospheres, have until recently severely limited the applicability of reliable ML relations to obtain robust MFs at the low-mass end.

3.1 The mass–luminosity relation down to $\sim 0.4\,\mathrm{M}_\odot$

As shown by equation (3), it is in fact the *slope* of the ML relation at a given absolute magnitude that determines the corresponding mass, which is therefore quite model dependent. This has been addressed in detail by, for example, D'Antona & Mazzitelli (1983), Kroupa et al. (Kroupa, Tout & Gilmore 1990; Kroupa et al. 1993), Elson et al. (1995) and Kroupa & Tout (1997).

The slope of the ML relation varies significantly with absolute magnitude, or mass. As shown by Kroupa et al. (1990, 1993) for solar-metallicity stars with masses $m \lesssim 1\,\mathrm{M}_\odot$, it has a local maximum at $M_V \approx 7$, and reaches a minimum at $M_V \approx 11.5$ (see also Kroupa 2000). This pronounced minimum corresponds to a maximum in the present-day LF, while the local maximum at $M_V \approx 7$ corresponds to the Wielen dip in the present-day LF of nearby stars (e.g. Kroupa et al. 1990; D'Antona & Mazzitelli 1996, and references therein).

The local maximum in the derivative of the ML relation at $M_V \approx 7$ ($m \approx 0.7\,\mathrm{M}_\odot$) is caused by the increased importance of the H^- opacity in low-mass stars with decreasing mass (KTG93; Kroupa & Tout 1997).

The ML relation steepens near $M_V = 10$ ($m \sim 0.4$–$0.5\,\mathrm{M}_\odot$), caused by the increased importance of H_2 formation in the outer shells of main-sequence stars, which in turn leads to core contraction (e.g. Chabrier & Baraffe 1997; Baraffe et al. 1998; Kroupa 2000).

Given the non-linear shape of the ML relation and the small slope at the low-mass end, any attempt to model the ML relation by either a polynomial fit or a power-law dependence will yield intrinsically unreliable MFs (cf. Elson et al. 1995; Chabrier & Méra 1997), in particular, in the low-mass regime. This model dependence is clearly illustrated by, for example, Ferraro et al. (1997), who compared the MFs for the GC NGC 6752 derived from a variety of different ML relations at that time available in the literature.

3.2 Age and metallicity dependence and corrections for binarity

The exact shape of the ML relation is sensitive to metallicity; metallicity changes affect the stellar spectral energy distribution and therefore the (absolute) magnitude in a given optical passband (cf. Brewer et al. 1993). In fact, it has been argued (cf. Baraffe et al. 1998) that, although the *V*-band ML relation is strongly metallicity-dependent, the *K*-band ML relation is only a very weak function of metal abundance, yielding similar *K*-band fluxes for $[\mathrm{M/H}] = -0.5$ and 0.0. Although the ML relation is currently relatively well-determined for solar-metallicity stars with $m \gtrsim 0.8\,\mathrm{M}_\odot$, at low metallicities the relation remains very uncertain. This is partially because of the lack of an empirical comparison, and to our still relatively poor understanding of the physical properties of these stars, although major efforts are currently under way to alleviate this latter problem (e.g. the recent work by the Lyon group).

Fortunately, as long as we only consider unevolved main-sequence stars, age effects are negligible and can therefore be ignored (cf. Brewer et al. 1993; Ferraro et al. 1997). This applies to the current study for the stellar mass range considered.

Finally, stellar populations contain in general at least 50 per cent of multiple systems. The immediate effect of neglecting a significant fraction of binary stars in our LF-to-MF conversion will be an underestimate of the resulting MF slope (cf. Fischer et al. 1998; Kroupa 2000). We will return to this point in Section 5.3.

3.3 A comparison of mass–luminosity relations

3.3.1 Luminosity-to-mass conversion for stars with masses below $1\,\mathrm{M}_\odot$

Since no empirical ML relations are available for low-mass, low-metallicity main-sequence stars, a test of the goodness of ML relations in this regime must therefore have a bearing on the comparison of different models. Several recent studies have adopted this approach (e.g. Alexander et al. 1997; Ferraro et al. 1997; Kroupa & Tout 1997; Piotto, Cool & King 1997; Saviane et al. 1998).

For solar-metallicity stars in the mass range $0.1 < m \leq 1\,\mathrm{M}_\odot$, Leggett et al. (1996) and Kroupa & Tout (1997) concluded that, although *all* models considered provided reasonable fits to the empirical ML relation, the theoretical ML relations of Baraffe et al. (1995) provided the best overall agreement with all recent observational constraints. On the other hand, Bedin et al. (2001) show that these are poor at low metallicity. It should be noted that the models of Baraffe et al. (1995) were based on *grey* model atmospheres.

Both Piotto et al. (1997) and Saviane et al. (1998), from a comparison of largely the same theoretical ML relations available in the literature with observational data for the low-metallicity Galactic GCs NGC 6397 ($[\mathrm{Fe/H}] \simeq -1.9$) and NGC 1851 ($[\mathrm{Fe/H}] \simeq -1.3$), respectively, concluded that the theoretical ML relations of Alexander et al. (1997) for the appropriate metallicity provided the best match for masses $m \lesssim 0.6$–$0.8\,\mathrm{M}_\odot$. Similar conclusions were drawn by Piotto et al. (1997) for three other Galactic GCs, M15, M30 and M92. Alexander et al. (1997) themselves found a good to excellent overall agreement between their models and those of the Lyon group, in particular, the updated ones of Chabrier, Baraffe & Plez (1996), which employ the most recent non-grey model atmospheres.

Fig. 1(a) shows the available empirical data, on which these comparisons are based for solar-metallicity stellar populations. The filled bullets represent the HM93 sample; the open circles the higher-mass Andersen (1991) binary stars. In panel (b), we show the $m \leq 2\,\mathrm{M}_\odot$ subsample. Overplotted are the best-fitting relation of HM93 (solid line), the fit to their semi-empirical ML relation (dotted line) of KTG93 and Kroupa & Tout (1997), and the theoretical ML relation of Chabrier et al. (1996, dashed line) for $0.075 \leq m \leq 0.6\,\mathrm{M}_\odot$. The figure shows that the observational data

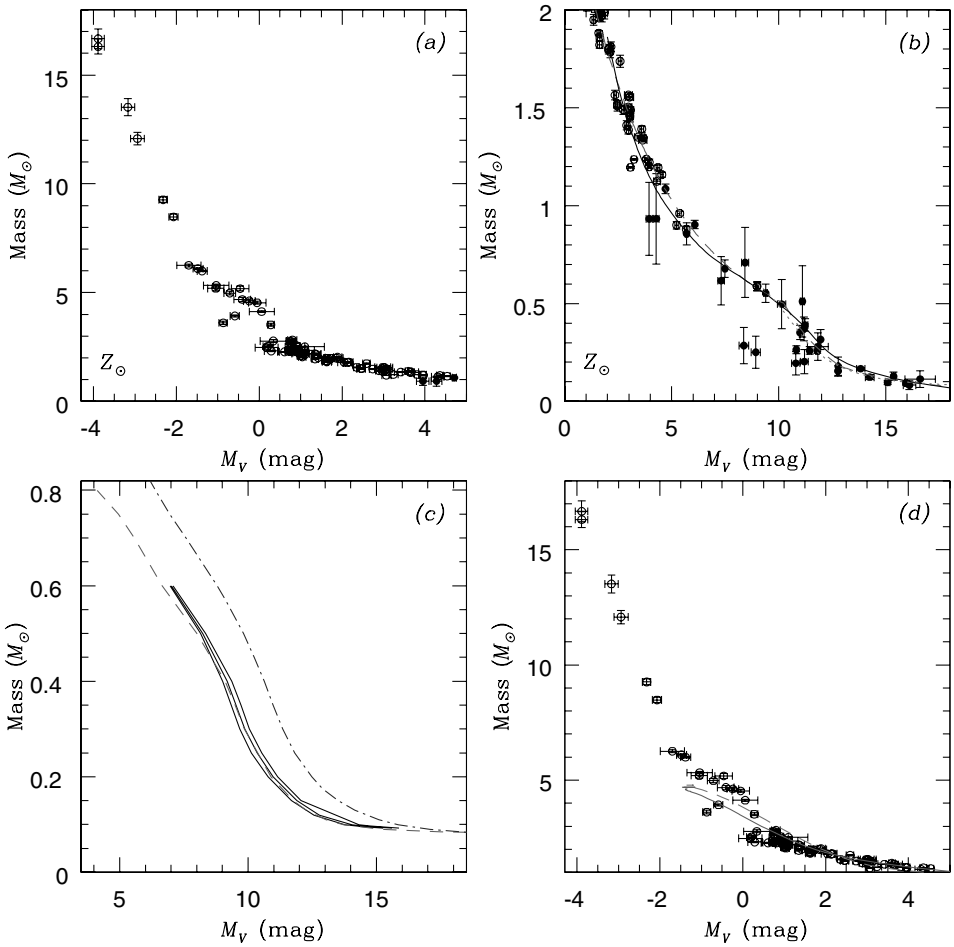

Figure 1. Empirical and theoretical ML relations: (a) solid bullets, HM93; open circles, Andersen (1991); (b) solid line, HM93 fit; dotted line, KTG93 and Kroupa & Tout (1997) semi-empirical ML relation; dashed line, Chabrier et al. (1996) theoretical ML relation for $m \leq 0.6\,\mathrm{M}_\odot$, based on a third-order polynomial fit; (c) theoretical ML relations for subsolar abundances, Alexander et al. [1997; solid lines, for [M/H] $= -1.3, -1.5, -2.0$ (top to bottom)] and Baraffe et al. (1997, dashed line, [M/H] $= -1.5$). For comparison, the solar-abundance ML relation of Baraffe et al. (1997) is also shown (dash-dotted line). (d) Observational data for $m \geq 1.0\,\mathrm{M}_\odot$ stars (Andersen 1991) and (for $m \leq 5\,\mathrm{M}_\odot$) theoretical models by GBBC00 for solar abundance (solid line) and [M/H] $= -1.3$ (dashed line).

allow for significant local differences in the slope of the solar-metallicity ML relation; these uncertainties propagate through the derivative of the relation when converting LFs to MFs.

The theoretical ML relation for solar abundance by Chabrier et al. (1996) closely follows the most recent semi-empirical ML relation compiled by Kroupa (KTG93; Kroupa & Tout 1997). In Fig. 1(c), we compare the current theoretical ML relations for subsolar metallicity: the solid lines represent the ML relations of Alexander et al. (1997) for (top to bottom) [M/H] $\simeq -1.3, -1.5$ and -2.0;[1] for reasons of clarity, we only show the [M/H] $= -1.5$ ML relation of Baraffe et al. (1997), but the spread caused by metallicity differences is similar to that shown by the relations of Alexander et al. (1997). The most significant differences between both sets of models are seen at masses $m \gtrsim 0.4\,\mathrm{M}_\odot$. This is likely to be caused by the slightly different treatment of the stellar atmospheres and radiative opacities. Finally, for comparison we also show the solar-metallicity theoretical ML relation of Chabrier et al. (1996) and Baraffe et al. (1997).

We plot the derivatives of the ML relations as a function of absolute visual magnitude in Fig. 2. From Fig. 2(a) it is immediately clear that the empirical fit to the HM93 ML relation inherently leads to unreliable luminosity-to-mass conversions because of the two sharp discontinuities in the slope.

Fig. 2(b) shows the metallicity dependence of the slope of the ML relation; the solid lines represent the ML relations of Alexander et al. (1997) with [M/H] $= -1.3, -1.5$ and -2.0, peaking from right to left. The models of Baraffe et al. (1997) (cf. the dashed line, for [M/H] $= -1.5$) closely follow those of Alexander et al. (1997). For comparison, we have also included the solar-abundance model of Chabrier et al. (1996) and Baraffe et al. (1997), as in panel (a).

3.3.2 The more massive stellar population

The main uncertainties for the luminosity evolution of stars with masses $m \gtrsim 0.8\,\mathrm{M}_\odot$ are in the treatment of the degree of mass loss

[1] We applied the procedure outlined in Ryan & Norris (1991) to convert the metallicities (Z) of Alexander et al. (1997) to [M/H] values: [M/H] $\approx$ [O/H] $=$ [O/Fe] $+$ [Fe/H], with [O/Fe] $= +0.35$ for [Fe/H] ≤ -1, and [O/Fe] $= -0.35 \times$ [Fe/H] for $-1 <$ [Fe/H] ≤ 0. Therefore, a stellar population with an observed [Fe/H] $= -1.5$ corresponds to a model with $[Z] = \log(Z/Z_\odot) = [M/H] \sim -1.15$, and $Z \simeq 1.35 \times 10^{-3}$. This procedure has been shown to apply to halo subdwarfs. These oxygen-enriched abundances are characteristic of old stellar populations in the Milky Way (cf. Baraffe et al. 1995). Gilmore & Wyse (1991) have shown that the element ratios in the LMC are significantly different, however.

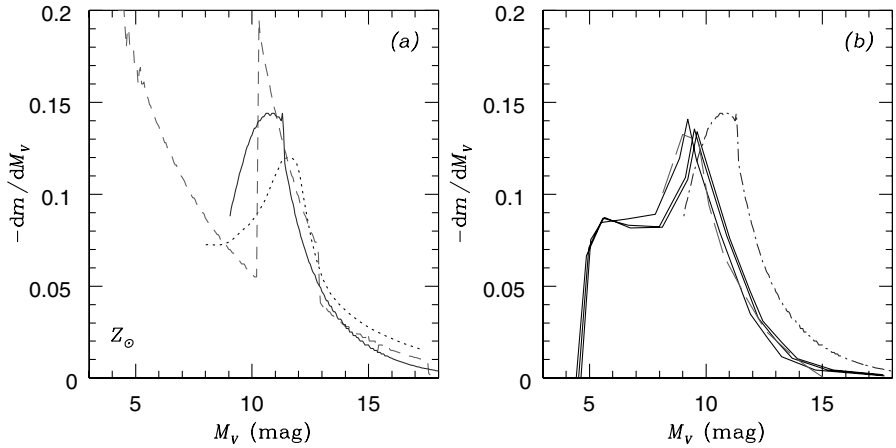

Figure 2. The slope of the ML relation. (a) Solar-metallicity ML relations, HM93 (dashed line, empirical), KTG93 and Kroupa & Tout (1997) (dotted line, semi-empirical) and Chabrier et al. (1996) and Baraffe et al. (1997) (solid line, theoretical); (b) theoretical ML relations for subsolar abundances, Alexander et al. [1997; solid lines, for [M/H] $= -1.3, -1.5, -2.0$ (peaking from right to left)], and Baraffe et al. (1997; dashed line, [M/H] $= -1.5$). For comparison, the solar-abundance ML relation of Chabrier et al. (1996) and Baraffe et al. (1997) is also shown (dash-dotted line, as in (a).

and convective core overshooting. Girardi et al. (2000, hereafter GBBC00) and Girardi (2001, private communication) computed a grid of stellar evolutionary models for stars in the mass range $0.15 \leq m \leq 7\,\mathrm{M}_\odot$ for metallicities between 1/50 and 1.5 times solar, using updated input physics and moderate core overshooting.

In Fig. 1(d), we show the observational ML relation of Andersen (1991) for stars with masses $m \geq 1.0\,\mathrm{M}_\odot$. In addition, we have plotted GBBC00's (2000) theoretical ML relations for solar metallicity (solid line) and for [M/H] $= -1.3$ (dashed line) for stars less massive than $\sim 5\,\mathrm{M}_\odot$. These models include moderate core overshooting, but the presence or absence of this process in the models does not significantly change the resulting ML relation for this mass range.

3.3.3 Comparison for our young LMC clusters

Based on the comparison and discussion in the previous sections, for the conversion of our observational (individual) stellar magnitudes (Paper I) to masses, and thence to MFs we will use the following.

(i) The empirical ML relation of HM93. This ML relation is defined for stars with $M_V \geq 1.45$.

(ii) The KTG93 and Kroupa & Tout (1997) semi-empirical ML relation for stars with $M_V \geq 2.00$, with an extension to $M_V = -3$ by adoption of Scalo's (1986) mass–M_V relation.

(iii) The parametrization of these by Tout et al. (1996, hereafter TPEH96), valid for masses in the range $-1 \leq \log m/\mathrm{M}_\odot \leq 2$; we converted the corresponding bolometric luminosities to absolute *V*-band magnitudes using the bolometric corrections of Lejeune, Cuisinier & Buser (1998). The TPEH96 ML relations are given as a function of metallicity from $Z = 10^{-4}$ to 0.03.

(iv) The GBBC00 models. For solar metallicities, the models for their youngest isochrone of 60 Myr are defined for stars with $-3.381 \leq M_V \leq 12.911$, while for the subsolar abundance of $Z = 0.008$ this corresponds to $-4.832 \leq M_V \leq 12.562$.

Although we argued that the models of Baraffe et al. (1998, hereafter BCAH98) employ the most recent input physics, their mass range, $m \lesssim 1.0\,\mathrm{M}_\odot$, precludes us from using their models, since completeness generally drops below our 50 per cent limit for $m \lesssim 0.8\,\mathrm{M}_\odot$, thus leaving us with too few data points for a useful comparison.

In Fig. 3 we compare the mass estimates based on HM93, KTG93, BCAH98 and GBBC00 with TPEH96's parametrization, for both solar and subsolar ([Fe/H] $= -0.5$) metallicities and ages of $\sim$10 and 25 Myr. Significant differences are seen among the individual models, in particular between TPEH96, on the one hand, and the high-mass end ($\log m/\mathrm{M}_\odot \gtrsim 0.3$) of KTG93 and between TPEH96 and the models of BCAH98, which show systematic deviations from the one-to-one relation indicated by the dashed line. It is therefore not unlikely that the differences among the models dominate the uncertainties in the derived MF and, ultimately, in the IMF slope (see also Bedin et al. 2001, who reached a similar conclusion in their analysis of the Galactic GC M4). We will quantify these effects in the next section.

In Fig. 4 we show examples of the derived global cluster MFs, normalized to unit area, for three of the ML conversions adopted in this paper, KTG93, TPEH96 and GBBC00. All MFs are shown for solar metallicity and for mass bins corresponding to luminosity ranges that exceed our 50 per cent completeness limits (see Paper I). The MFs, and all other MFs discussed in this paper, were corrected for incompleteness and background contamination following identical procedures as for the LFs in Paper I. Significant systematic effects result from the adoption of any given ML conversion, as can be clearly seen. For comparison, we also plot a fiducial Salpeter IMF, which appears to be a reasonable approximation for the global cluster MFs in the mass range ($-0.15 \lesssim \log m/\mathrm{M}_\odot \lesssim 0.8$).

4 QUANTIFICATION OF MASS SEGREGATION EFFECTS

4.1 Radial dependence of luminosity and mass functions

The effects of mass segregation can be quantified using a variety of methods. The most popular and straightforward diagnostic for mass segregation effects is undoubtedly the dependence of the MF slope, $\Gamma = \Delta\log\xi(m)/\Delta m$ [where $\xi(m) \propto m^\Gamma$], on the cluster radius.

In Fig. 5 we plot the derived MF slopes as a function of the cluster radius for our four adopted ML conversions and assuming three different fitting ranges in mass:

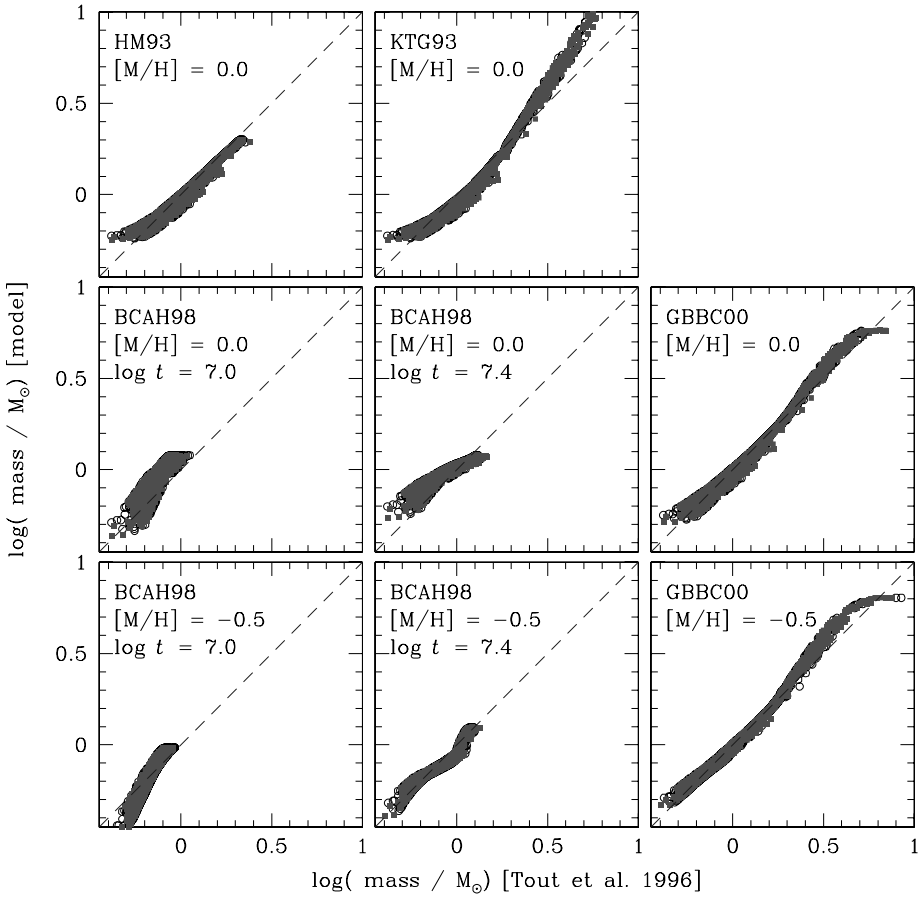

Figure 3. Comparison of the mass estimates for NGC 1805 (open circles) and NGC 1818 (filled circles) resulting from various ML relations. We used TPEH96's parametrization as comparison ML relation because of its large mass range.

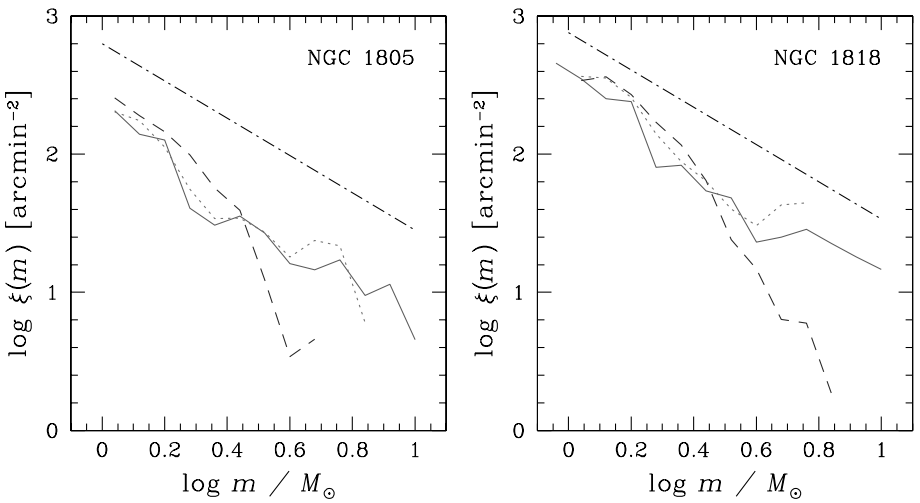

Figure 4. Examples of the derived global cluster MFs, normalized to unit area, for three of the ML conversions adopted in this paper, KTG93 (solid lines), TPEH96 (dashed lines) and GBBC00 (dotted lines). All MFs are shown for solar metallicity and for mass bins corresponding to luminosity ranges that exceed our 50 per cent completeness limits (see text). The dash-dotted lines show the Salpeter IMF corresponding to the mass range under consideration.

(i) $-0.15 \leq \log m/\mathrm{M}_{\odot} \leq 0.30$ for all conversions;

(ii) $-0.15 \leq \log m/\mathrm{M}_{\odot} \leq 0.70$ for KTG93, TPEH96 and GBBC00; and

(iii) $-0.15 \leq \log m/\mathrm{M}_{\odot} \leq 0.85$ for TPEH96 and GBBC00.

The adopted radial ranges for our annular MFs are indicated by the horizontal bars at the bottom of each panel. Although we see a large spread among models and mass fitting ranges, clear mass segregation is observed in both clusters at radii $r \lesssim 20$ arcsec, well outside the cluster core radii (indicated by the vertical dotted lines). We have also indicated the Salpeter (1955) IMF slope, $\Gamma = -1.35$ (dashed horizontal lines). While both the global MFs (which are

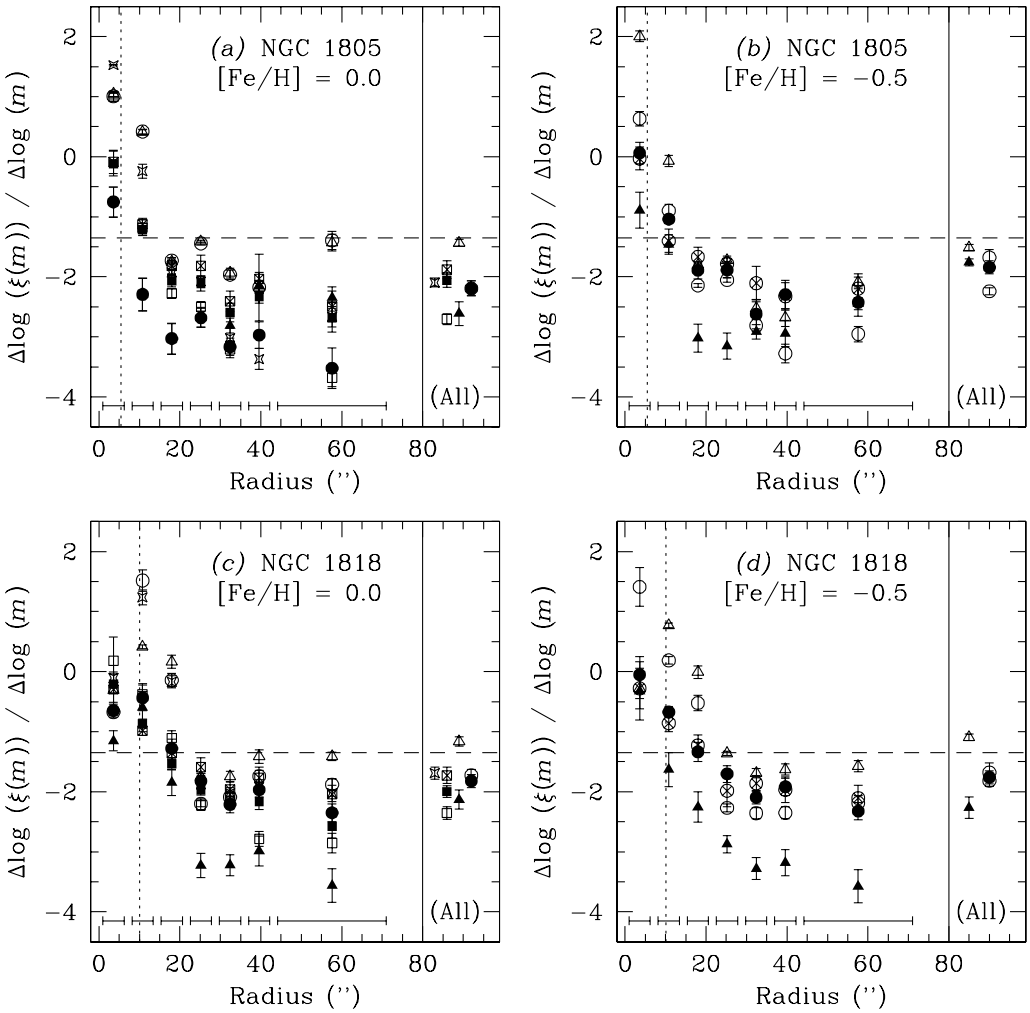

Figure 5. Mass function slopes as a function of cluster radius. The symbols are coded as follows: stars, HM93; squares, KTG93; triangles, TPEH96; circles, GBBC00; open symbols correspond to a mass range $-0.15 \leq \log m/\mathrm{M}_\odot \leq 0.30$, filled symbols to $-0.15 \leq \log m/\mathrm{M}_\odot \leq 0.70$ and crossed open symbols extend up to $\log m/\mathrm{M}_\odot = 0.85$. The vertical dotted lines indicate the cluster core radii; the Salpeter slope is represented by the horizontal dashed lines. The radial ranges over which the MF slopes were determined are shown by horizontal bars at the bottom of each panel. The right-hand subpanels show the overall MF slopes for the clusters as a whole; the data points are spread out radially for display purposes.

dominated by the inner, mass-segregated stellar population) and the annular MFs near the core radii appear to be consistent with the Salpeter IMF slope (cf. Vesperini & Heggie 1997; for the cluster models assumed here, $R_{\rm core} \approx R_{\rm h}$), the MFs beyond the cluster radii where mass segregation is significant (i.e. $r \gtrsim 30$ arcsec) are characterized by steeper slopes, i.e. relatively more low-mass stars compared with high-mass stars than found in the inner cluster regions. This result holds for all mass fitting ranges, all ML conversions considered, solar and subsolar ([Fe/H] $= -0.5$) metallicity and both clusters.

The error bars in Fig. 5 represent the formal uncertainty in the fits; the systematic uncertainties are clearly greater, and a strong function both of the adopted ML conversion and of the mass range used for the fitting of the MF slopes. In all cases, the larger mass ranges used for the fitting result in steeper MF slopes than the smaller (lowest-mass) range, thus presenting clear evidence for non-power-law-shaped MFs. In addition, the TPEH96 parametrization results in systematically steeper slopes for all cluster–metallicity combinations.

Because of the strong model dependence, in particular because of the sensitivity to the choice of ML relation, and the accuracy of the corrections for incompleteness and background star contamination of single power-law fits to the annular MFs, in Fig. 6 we introduce a more robust characterization of the presence of mass segregation in these two young star clusters. We quantified the deviations of the high-mass range of the annular MFs from the global MF following a similar procedure as defined in Paper I for the LFs. All annular MFs were normalized to the global MF in the range $0.00 \leq \log m/\mathrm{M}_\odot \leq 0.20$, where the effects of mass segregation – if any – are negligible, as shown above. Subsequently, we determined the sum of the differences between the global and the scaled annular MFs in the common mass range $0.20 < \log m/\mathrm{M}_\odot \leq 0.60$, $\Sigma(\Delta\Gamma)$. We adopted $\log m/\mathrm{M}_\odot = 0.60$ as an upper mass limit, so that we could compare the results of all three ML conversions.

From Fig. 6, it follows that both clusters are mass segregated within $R \simeq 30$ arcsec; beyond, the deviations become relatively constant with increasing radius. It is also clear (i) that there is no appreciable difference between the strength of the mass segregation in the two clusters and (ii) that the scatter among the data points from the different models is relatively small. We therefore conclude that we have been able to quantify the effects of

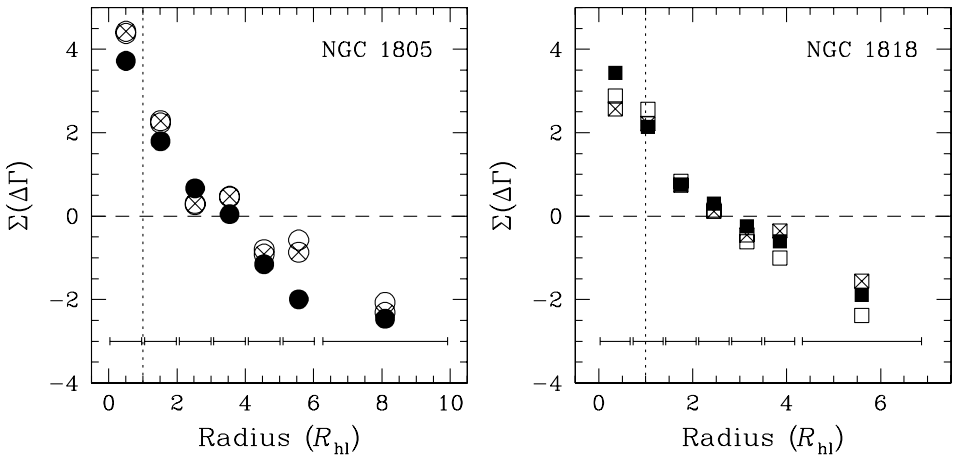

Figure 6. Deviations of the annular MFs from the global MF as a function of radius, as discussed in the text. Filled symbols were obtained using the ML relation of KTG93, open symbols are based on TPEH96's ML conversion, and crossed open symbols result from the GBBC00 models. The horizontal bars at the bottom of the figure indicate the radial range used to obtain the data points, the cluster core radii are indicated by the vertical dotted lines.

mass segregation in a fairly robust way by minimizing the effects of the choice of ML conversion.

It is most likely that the effect referred to as mass segregation is indeed caused by a positional dependence of the ratio of high-mass to low-mass stars within the clusters, and not to different age distributions ('age segregation'). Johnson et al. (2001) have shown that for the high-mass stars in both clusters the LF is indeed just a smoothed (almost) coeval CMD, for which age effects are only of second-order importance. It is possible that for very low stellar masses, i.e. pre-main-sequence stars, age segregation may play a more important role, but this applies only to stars well below the 50 per cent completeness limits for both clusters.

Finally, we point out that it is generally preferred to use star counts rather than surface brightness profiles to measure mass segregation effects (e.g. Elson et al. 1987b; Chernoff & Weinberg 1990). Elson et al. (1987b) argue that the use of surface brightness profiles by themselves, although initially used to study mass segregation (e.g. da Costa 1982; Richer & Fahlman 1989), is limited in the sense that one cannot distinguish between these effects and any significant degree of radial velocity anisotropy in the outer regions of a cluster (see also Chernoff & Weinberg 1990). In addition, a comparison between results obtained from star counts and from surface brightness profiles does not necessarily trace the same system, since star counts are generally dominated by main-sequence (and subgiant-branch) stars, while surface brightness profiles mostly trace the giants (and also subgiant stars) in a cluster (cf. Elson et al. 1987b).

4.2 Core radii

Conclusive results on the presence of mass segregation in clusters can also be obtained by examining the core radii of specific massive stellar species (e.g. Brandl et al. 1996), or – inversely – by measuring the mean stellar mass within a given radius (e.g. Bonnell & Davies 1998; Hillenbrand & Hartmann 1998). However, it may not always be feasible to use this diagnostic, since the individual stellar masses of the cluster members need to be known accurately, thus providing an additional observational challenge. In addition, the results depend critically on which stars are used to obtain the mean mass, and can be severely affected by small-number statistics (cf. Bonnell & Davies 1998).

Fig. 7 and Table 1 show the dependence of the derived cluster core radius on the adopted magnitude (or mass) range. Core radii were derived based on fits to stellar number counts – corrected for the effects of incompleteness[2] and background contamination (cf. Paper I) – of the generalized fitting function proposed by Elson et al. (1987a), in the linear regime:

$$\mu(r) = \mu_0 \left[1 + \left(\frac{r}{a}\right)^2\right]^{-\gamma/2}, \qquad (4)$$

where $\mu(r)$ and μ_0 are the radial and central surface brightness, respectively, γ corresponds to the profile slope in the outer regions of the cluster, and $R_{\rm core} \approx a(2^{2/\gamma} - 1)^{1/2} \approx R_{\rm h}$. Equation (4) reduces to a modified Hubble law for $\gamma = 2$, which is a good approximation to the canonical King model for GCs (King 1966).

For both NGC 1805 and 1818 we clearly see the effects of mass segregation for stars with masses $\log m/{\rm M}_\odot \gtrsim 0.2$ ($M_V \lesssim 2.4; m \gtrsim 1.6\,{\rm M}_\odot$). It is also clear that the brightest four magnitude ranges, i.e. masses $\log m/{\rm M}_\odot \gtrsim 0.4 (m \gtrsim 2.5\,{\rm M}_\odot)$, show a similar concentration, while a trend of increasing core radius with decreasing mass (increasing magnitude) is apparent for lower masses. The larger scatter for NGC 1818 is caused by the smaller number of stars in each magnitude bin compared with NGC 1805. For NGC 1818 the associated uncertainties are determined by a combination of the scatter in the derived core radii and background effects, while the uncertainties for NGC 1805 are dominated by the effects of background subtraction.

We have also indicated the core radii obtained from profile fits to the overall surface brightness profiles of the clusters. It is clear that these are dominated by the mass-segregated high-mass (bright) stars.

5 A COMPARISON OF MASS FUNCTION SLOPES – TRACING THE IMF?

5.1 Comparison with previously published results

Few studies have published MFs of sufficient detail and quality for the two young LMC clusters analysed in this paper to allow useful comparisons. Santiago et al. (2001) published global MFs and MFs determined in the annulus $4.9 < R < 7.3$ pc ($19.4 < R < 28.8$ arcsec) for both NGC 1805 and 1818, based on the same

[2] We have only used magnitude (mass) ranges for which the completeness fractions, as determined in Paper I, were at least 50 per cent.

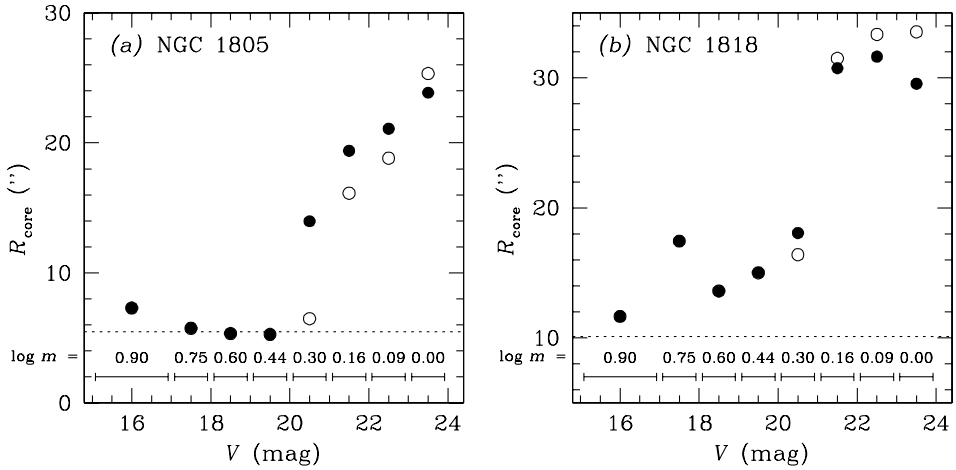

Figure 7. Core radii as a function of magnitude (mass). The filled circles are the core radii after correction for the effects of (in)completeness, area covered by the observations, and background stars; the open circles are not background subtracted and serve to indicate the uncertainties caused by background correction. We have also indicated the mean cluster core radii, obtained from surface brightness profile fits (dotted lines). The horizontal bars at the bottom of the panels indicate the magnitude ranges used to obtain the core radii; the numbers indicate the approximate mass (in $M_\odot$) corresponding to the centre of each magnitude range.

Table 1. Cluster core radii as a function of mass.

Magnitude range (V)	$\log m/M_\odot$ (central)	NGC 1805 (arcsec)	(pc)	NGC 1818 (arcsec)	(pc)
15.0–17.0	0.90	7.30	1.85	11.65	2.95
17.0–18.0	0.75	5.74	1.45	17.45	4.41
18.0–19.0	0.60	5.34	1.35	13.61	3.44
19.0–20.0	0.44	5.27	1.33	15.01	3.80
20.0–21.0	0.30	13.97	3.53	18.07	4.57
21.0–22.0	0.16	19.39	4.91	30.74	7.78
22.0–23.0	0.09	21.09	5.34	31.63	8.00
23.0–24.0	0.00	23.86	6.04	29.55	7.48
15.0–24.0		16.96	4.29	23.92	6.05

Note. The range ($15.0 \leq V \leq 24.0$) represents the cluster average, corrected for completeness, area covered by the observations and the background population.

observations used for the present study, while Hunter et al. (1997) published the global MF and the core MF derived from the *HST* WFPC2/PC chip of NGC 1818. In Fig. 8 we compare our results with those of Hunter et al. (1997) and Santiago et al. (2001).

Although Santiago et al. (2001) used a different ML conversion than used in the present paper, the slopes and the dependence on the adopted mass fitting range they derived for their annular MFs are fully consistent with the range seen at this radius, using any of the ML relations employed by us. However, their and Hunter et al.'s (1997) global MF slopes are somewhat shallower than ours. The difference is sufficiently small, however, that it can be explained as being caused by the combination of different ML relations and a different treatment of the background stellar population (see Paper I for a discussion of the latter). Hunter et al. (1997) found no significant difference in MF slope between the core MF ($\Gamma = -1.21 \pm 0.10$) and the global MF ($\Gamma = -1.25 \pm 0.08$), in the mass range between 0.85 and 9 $M_\odot$ ($-0.07 \lesssim \log m/M_\odot \lesssim 0.95$). The PC field of view samples the inner $r \sim 18$ arcsec; we have also included their core data point in Fig. 8. Although the PC MF slope of Hunter et al. (1997) appears to be slightly steeper than most of our MF slope determinations at these radii, this can easily be explained as being caused by a combination of the uncertainties in the ML conversion used (as demonstrated by the range in MF slopes seen in Fig. 5) and the intrinsic curvature of the MF. From Fig. 5 it follows that the MF slopes become steeper if increasingly higher-mass stars are included in the fitting range (compare the location of the open, filled and open-crossed symbols, which indicate increasing mass fitting ranges). The PC MF slope determination of Hunter et al. (1997) is based on a mass range extending up to 9 $M_\odot$, while our largest fitting range only includes stars $\lesssim 7\,M_\odot$. The observed curvature in the MF will therefore result in a slightly steeper slope for the MF slope of Hunter et al. (1997), although still fairly similar to the slopes determined using our greatest mass fitting ranges at these radii (cf. Fig. 8).

With regard to the use of different ML relations, it is worth noting here that the difference between the MF slopes derived by us and those of both Hunter et al. (1997) and Santiago et al. (2001) may be largely because of the adopted isochrones: while for older clusters the MF slopes for main-sequence stars are almost independent of age, small differences between MF slopes as a function of age are appreciated for younger stellar populations. This difference is in the sense that using isochrones for older stellar populations will result in slightly shallower MF slopes. This is the most likely explanation for the slight shift between our MF slopes (based on solar neighbourhood-type stellar populations) and those of Hunter et al. (1997) and Santiago et al. (2001), who both used

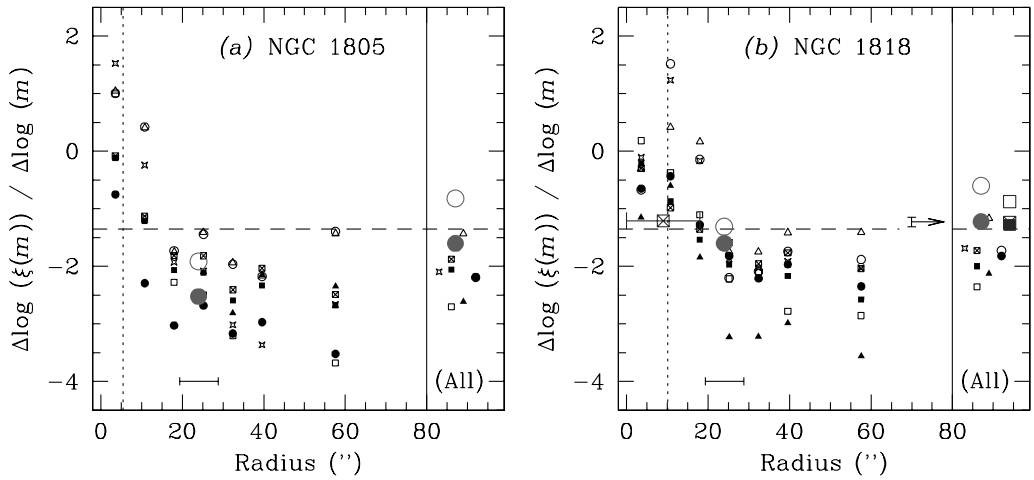

Figure 8. Comparison of MF slopes. The small symbols represent our NGC 1805 and 1818 data points; the symbol and line coding is as in Fig. 5. The large circles represent the MF slopes of Santiago et al. (2001); the large squares those of Hunter et al. (1997) for NGC 1818, while the symbol coding is as for the small symbols. The radial ranges are again indicated by the horizontal bars in each panel. The arrow with vertical error bar in the panel of NGC 1818 (located at $r = 70$ arcsec) shows the global MF slope derived by Hunter et al. (1997) and its associated 1σ uncertainty. Solar abundances were assumed.

younger isochrones to obtain their mass estimates. However, the expected steepening in MF slope from evolved to young stellar populations is almost entirely contained within the observed spread in MF slope in both clusters (cf. Hunter et al. 1997). In fact, for the ML conversion based on the GBBC00 models, we used their youngest isochrone (at $t = 6 \times 10^7$ yr); the resulting MFs are shown as circles in Fig. 5. Hunter et al. (1997) showed that if they had used a 30–40 Myr isochrone instead of the one at 20 Myr used by these authors, it would make the IMF slope appear *shallower* by $\Delta\Gamma \sim 0.15$. Thus, it appears that the GBBC00 slopes are entirely consistent with the slopes obtained from the other ML relations, however, which emphasizes our statement that any slope difference caused by the adoption of different isochrones is accounted for by the observed spread in MF slopes.

A further comparison is provided by the result of Will et al. (1995), who obtained an MF slope of $\Gamma = -1.1 \pm 0.3$ for stars between 2 and 8 $M_\odot$ (or $\log m/M_\odot = 0.30-0.90$). This slope is significantly shallower than any of the slopes derived by us, in particular in view of the observed steepening of the MF slope when including increasingly higher-mass stars (Section 4.1). A similar discrepancy was already noted by Hunter et al. (1997), who argued that this difference (and their greater uncertainties) was most probably caused by the difficulty in obtaining reliable photometry from crowded ground-based images, while they were not able to resolve stars in the cluster centre, nor detect stars of similarly faint magnitudes (low masses) as possible with *HST* observations.

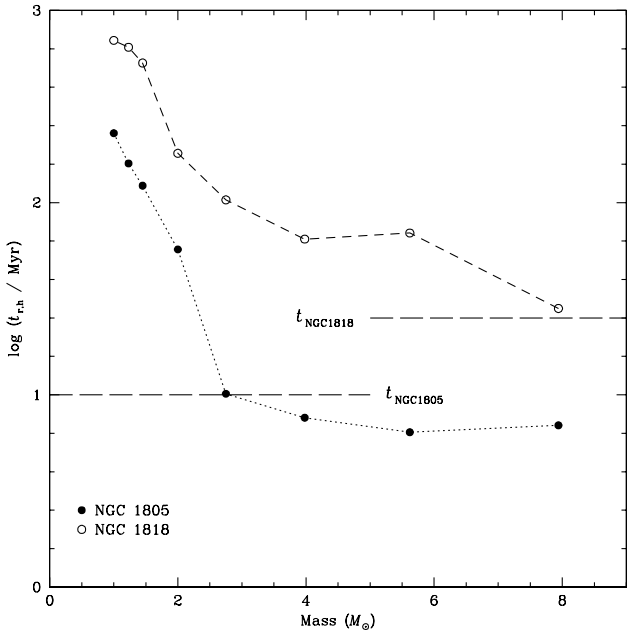

Figure 9. Half-mass relaxation time as a function of mass for NGC 1805 and 1818. The best age estimates for both clusters are indicated by horizontal dashed lines.

5.2 Primordial or dynamical mass segregation?

The key question is whether the observed mass segregation in both young LMC star clusters is the result of the process of star formation itself or caused by dynamical relaxation. In Fig. 9 we have plotted the half-mass relaxation time as a function of mass, using equation (1) and the mass-dependent core radii of Fig. 7. For comparison, we have also indicated the ages of both clusters. For NGC 1805 significant dynamical mass segregation is expected to have occurred out to its half-mass radius for stars more massive than $\sim 3\,M_\odot$ ($\log m/M_\odot \simeq 0.48$), while for NGC 1818 this corresponds to stars exceeding $\sim 8\,M_\odot$ ($\log m/M_\odot \gtrsim 0.90$). However, from Fig. 7 it follows that mass segregation becomes significant for masses $m \gtrsim 2.5\,M_\odot$, out to at least 20–30 arcsec, or $3-6R_{\rm core}$.

Dynamical mass segregation in the cluster cores will have occurred on 10–20 times shorter time-scales, in particular for the more massive stars (cf. equation 2). In fact, if the cluster contains a significant amount of gas, for example, $M_{\rm gas} \gtrsim M_{\rm stars}$ (cf. Lada 1991; Bonnell & Davies 1998), this will increase the gravitational potential of the cluster, and thus the virialized stellar velocity dispersion (Bonnell & Davies 1998). Therefore, in this case a larger number of two-body encounters, and hence time, is required to reach a dynamically relaxed state. Thus, the relaxation time estimates obtained by considering only the contributions of the stellar component of the cluster should be considered lower limits, especially for young star clusters, which are generally rich in gas.

Elson et al. (1987b) estimated the central velocity dispersion in NGC 1818 to be in the range $1.1 \lesssim \sigma_0 \lesssim 6.8\,\mathrm{km\,s^{-1}}$. Combining this central velocity dispersion, the core radius of $\simeq$2.6 pc, and the cluster age of $\simeq$25 Myr, we estimate that the cluster core is between $\sim$5 and $\sim$30 crossing times old, so that dynamical mass segregation in the core should be well under way. Although we do not have velocity dispersion information for NGC 1805, it is particularly interesting to extend this analysis to this younger ($\sim$10-Myr) cluster. We know that its core radius is roughly half that of NGC 1818, and its mass is a factor of $\sim$10 smaller. Simple scaling of equation (1) then shows that the half-mass relaxation time of NGC 1805 is $\sim$4–5 times as short as that of NGC 1818; if we substitute the scaling laws into equation (2), we estimate that the central velocity dispersion in NGC 1805 is $\gtrsim$10 times smaller than that in NGC 1818. From this argument it follows that the cluster core of NGC 1805 is $\lesssim$3–4 crossing times old.

However, since strong mass segregation is observed out to $\sim 6R_{\rm core}$ and $\sim 3R_{\rm core}$ in NGC 1805 and 1818, respectively, for stellar masses in excess of $\sim$2.5 $\mathrm{M}_\odot$, it is most likely that significant primordial mass segregation was present in both clusters, particularly in NGC 1805. Although this was initially suggested by Santiago et al. (2001), we have now substantiated this claim quantitatively. Relevant to this discussion is the study by Bonnell & Davies (1998), who found that whenever a system of massive stars is found at the centre of a young star cluster, such as the Trapezium stars in the ONC, a major fraction of it most probably originated in the inner parts of the cluster. *N*-body simulations are currently being carried out to investigate the fraction of massive stars, and their mass range, that will have to have originated in the cluster centres to result in the observed distribution. We will include these in a subsequent paper (de Grijs et al., in preparation).

5.3 The slope of the cluster mass function

We will now return to the discussion of Figs 5 and 8. In Section 4.1 we showed (i) that the slope of the global cluster MF is relatively well approximated by that at the cluster core radius; (ii) that at the cluster core radius the effects of strong mass segregation are still clearly visible; and (iii) that in the outer cluster regions, the slope of the (annular) cluster MFs approaches a constant value.

Within the uncertainties, we cannot claim that the slopes of the outer MFs in NGC 1805 and 1818 are significantly different. Starting with the work by Pryor et al. (1986) and McClure et al. (1986), it is expected that clusters with similar metallicities exhibit similar MF slopes. However, Santiago et al. (2001) claimed to have detected a significantly different MF slope for both the global and their annular MF between both clusters. As is clear from Fig. 8, their annular MFs were not taken at sufficiently large radii to avoid the effects of mass segregation. Since both clusters are affected by mass segregation in a slightly different way (which may just be a reflection of the difference in their dynamical ages), it is not surprising that the annular MFs of Santiago et al. (2001) exhibit different slopes.

Recent studies show that the actual value of the MF slope may vary substantially from one region to another, depending on parameters such as the recent star formation rate, metallicity and mass range (cf. Brandl et al. 1996). The outer cluster regions of R136/30Dor (Malumuth & Heap 1994; Brandl et al. 1996), M5 (Richer & Fahlman 1987), M15 (Sosin & King 1997) and M30 (Sosin 1997) are all characterized by MF slopes $\Gamma \lesssim 2.0$. Bonnell et al. (2001b) explain this rather steep MF slope naturally as being caused by the process of star formation and accretion itself, resulting from the combination of a gas-dominated and a stellar-dominated regime within the forming cluster. This results in a double-power-law IMF, where the lower-mass stars have a shallower slope and the high-mass IMF slope is steeper ($\Gamma \approx -1.5$ and $-2 \leq \Gamma \lesssim -2.5$, respectively), caused by the different accretion physics operating in each regime (i.e. tidal-lobe accretion versus Bondi–Hoyle accretion for low- and high-mass stars, respectively).

As mentioned in Section 3.2, if there is a significant percentage of binary or multiple stars in a star cluster, this will lead us to an underestimate of the MF slope. In other words, the MF slopes determined in this paper are lower limits, because we have assumed that all stars detected in both clusters are single stars. Elson et al. (1998) found a fraction of $\sim 35 \pm 5$ per cent of roughly similar mass binaries (with the mass of the primary $\sim$2–5.5 $\mathrm{M}_\odot$) in the centre of NGC 1818, decreasing to $\sim 20 \pm 5$ per cent in the outer regions of the cluster, which they showed to be consistent with dynamical mass segregation. It is not straightforward to correct the observed LFs for the presence of binaries, in particular since the binary fraction as a function of brightness is difficult to determine. If we consider the information at hand, (i) the small ($\sim$15 per cent) gradient in the total binary fraction derived by Elson et al. (1998) for the inner $\sim$3 core radii of NGC 1818; (ii) the result of Rubenstein & Bailyn (1999) that the binary fraction increases at fainter magnitudes in the Galactic GC NGC 65752; and (iii) the similarity of our annular LFs for faint magnitudes for all annuli and both clusters, we conclude that the effects of a binary population in either or both of NGC 1805 and 1818 are likely to be smaller than the observed differences in LF shapes as a function of radial distance from the cluster centres. This is corroborated by the result of Elson et al. (1998) for NGC 1818.

6 SUMMARY AND CONCLUSIONS

We have reviewed the complications involved in the conversion of observational LFs into robust MFs, which we have illustrated using a number of recently published ML relations. These ML relations were subsequently applied to convert the observed LFs of NGC 1805 and 1818, the two youngest star clusters in our *HST* programme of rich compact LMC star clusters, into MFs.

The radial dependence of the MF slopes indicate clear mass segregation in both clusters at radii $r \lesssim 20$–30 arcsec, well outside the cluster core radii. This result does not depend on the mass range used to fit the slopes or the metallicity assumed. In all cases, the larger mass ranges used for the fitting result in steeper MF slopes than the smallest mass range dominated by the lowest-mass stars, thus presenting clear evidence for non-power-law-shaped MFs. Within the uncertainties, we cannot claim that the slopes of the outer MFs in NGC 1805 and 1818 are significantly different. We also argue that our results are consistent with previously published results for these clusters if we properly take the large uncertainties in the conversion of LFs to MFs into account. The MF slopes obtained in this paper are in fact lower limits if there is a significant fraction of binary stars present in the clusters.

The global cluster MFs (which are dominated by the inner, mass-segregated stellar population) and the annular MFs near the core radii appear to be characterized by similar slopes, the MFs beyond the cluster radii where mass segregation is significant (i.e. $r \gtrsim$ 30 arcsec) are characterized by steeper slopes. It is, however, not unusual for star clusters to be characterized by rather steep MF slopes; Bonnell et al. (2001b) explain this naturally as being caused

by the different accretion physics operating in the low- and high-mass star-forming regime.

We analysed the dependence of the cluster core radius on the adopted magnitude (mass) range. For both clusters we clearly detect the effects of mass segregation for stars with masses $\log m/\mathrm{M}_\odot \gtrsim 0.2$ ($m \gtrsim 1.6\,\mathrm{M}_\odot$). It is also clear that stars with masses $\log m/\mathrm{M}_\odot \gtrsim 0.4$ ($m \gtrsim 2.5\,\mathrm{M}_\odot$) show a similar concentration, while a trend of increasing core radius with decreasing mass (increasing magnitude) is apparent for lower masses. The characteristic cluster core radii, obtained from profile fits to the overall surface brightness profiles, are dominated by the mass-segregated high-mass stars.

We estimate that the NGC 1818 cluster core is between $\sim$5 and $\sim$30 crossing times old, so that dynamical mass segregation in its core should be well under way. Although we do not have velocity dispersion information for NGC 1805, by applying scaling laws we conclude that its core is likely to be $\lesssim$3–4 crossing times old. However, since strong mass segregation is observed out to $\sim 6R_{\mathrm{core}}$ and $\sim 3R_{\mathrm{core}}$ in NGC 1805 and 1818, respectively, for stellar masses in excess of $\sim 2.5\,\mathrm{M}_\odot$, it is most likely that significant primordial mass segregation was present in both clusters, particularly in NGC 1805. We are currently investigating this further using *N*-body simulations.

ACKNOWLEDGMENTS

We thank Christopher Tout and Mark Wilkinson for useful discussions and Isabelle Baraffe for making unpublished subsolar metallicity model results from her NEXTGEN code available to us. We acknowledge insightful and constructive comments by the referee. This paper is based on observations with the NASA/ESA *Hubble Space Telescope*, obtained at the Space Telescope Science Institute, which is operated by the Association of Universities for Research in Astronomy (AURA), Inc., under NASA contract NAS 5-26555. This research has made use of NASA's Astrophysics Data System Abstract Service.

REFERENCES

Aarseth S. J., 1999, PASP, 111, 1333
Aarseth S. J., Heggie D. C., 1998, MNRAS, 297, 794
Alexander D. R., Brocato E., Cassisi S., Castellani V., Ciacio F., Degl'Innocenti S., 1997, A&A, 317, 90
Andersen J., 1991, A&AR, 3, 91
Bedin L. R., Anderson J., King I. R., Piotto G., 2001, ApJ, 560, L75
Bica E., Alloin D., Santos J. F. C., Jr, 1990, A&A, 235, 103
Baraffe I., Chabrier G., Allard F., Hauschildt P. H., 1995, ApJ, 446, L35
Baraffe I., Chabrier G., Allard F., Hauschildt P. H., 1997, A&A, 327, 1054
Baraffe I., Chabrier G., Allard F., Hauschildt P. H., 1998, A&A, 337, 403 (BCAH98)
Barbaro G., Olivi F. M., 1991, AJ, 101, 922
Bedin L. R., Anderson J., King I. R., Piotto G., 2001, ApJ, 560, L75
Bonatto C., Bica E., Alloin D., 1995, A&AS, 112, 71
Bonnell I. A., Davies M. B., 1998, MNRAS, 295, 691
Bonnell I. A., Bate M. R., Clarke C. J., Pringle J. E., 1997, MNRAS, 285, 201
Bonnell I. A., Bate M. R., Zinnecker H., 1998, MNRAS, 298, 93
Bonnell I. A., Bate M. R., Clarke C. J., Pringle J. E., 2001a, MNRAS, 323, 785
Bonnell I. A., Clarke C. J., Bate M. R., Pringle J. E., 2001b, MNRAS, 324, 573
Brandl B. et al., 1996, ApJ, 466, 254
Brewer J. P., Fahlman G. G., Richer H. B., Searle L., Thompson I., 1993, AJ, 105, 2158
Bruzual G., Charlot S., 1996, in Leitherer C. et al., eds, PASP, 108, 996 (AAS CDROM Series 7)
Cassatella A., Barbero J., Brocato E., Castellani V., Geyer E. H., 1996, ApJS, 102, 57
Chabrier G., Baraffe I., 1997, A&A, 327, 1039
Chabrier G., Méra D., 1997, A&A, 328, 83
Chabrier G., Baraffe I., Plez B., 1996, ApJ, 459, L91
Chernoff D. F., Weinberg M. D., 1990, ApJ, 351, 121
Da Costa G. S., 1982, AJ, 87, 990
D'Antona F., Mazzitelli I., 1983, A&A, 127, 149
D'Antona F., Mazzitelli I., 1996, ApJ, 456, 329
de Grijs R., Johnson R. A., Gilmore G. F., Frayn C. M., 2002, MNRAS, 331, 228 (Paper I, this issue)
De Marchi G., Paresce F., 1996, ApJ, 467, 658
Elson R. A. W., Fall S. M., Freeman K. C., 1987a, ApJ, 323, 54
Elson R. A. W., Hut P., Inagaki S., 1987b, ARA&A, 25, 565
Elson R. A. W., Gilmore G. F., Santiago B. X., Casertano S., 1995, AJ, 110, 682
Elson R. A. W., Sigurdsson S., Davies M. B., Hurley J., Gilmore G. F., 1998, MNRAS, 300, 857
Fabregat J., Torrejón J. M., 2000, A&A, 357, 451
Ferraro F. R., Carretta E., Bragaglia A., Renzini A., Ortolani S., 1997, MNRAS, 286, 1012
Fischer P., Pryor C., Murray S., Mateo M., Richtler T., 1998, AJ, 115, 592
Gilmore G., Wyse R. F. G., 1991, ApJ, 367, L55
Girardi L., Bressan A., Bertelli G., Chiosi C., 2000, A&AS, 141, 371 (GBBC00)
Grebel E. K., 1997, A&A, 317, 448
Henry T. J., McCarthy D. W., 1993, AJ, 106, 773 (HM93)
Hillenbrand L. A., Hartmann L. E., 1998, ApJ, 492, 540
Hunter D. A., Shaya E. J., Holtzman J. A., Light R. M., O'Neil E. J., Lynds R., 1995, ApJ, 448, 179
Hunter D. A., Light R. M., Holtzman J. A., Lynds R., O'Neil E. J., Jr, Grillmair C. J., 1997, ApJ, 478, 124
Inagaki S., Saslaw W. C., 1985, ApJ, 292, 339
Jasniewicz G., Thévenin F., 1994, A&A, 282, 717
Johnson R. A., Beaulieu S. F., Gilmore G. F., Hurley J., Santiago B. X., Tanvir N. R., Elson R. A. W., 2001, MNRAS, 324, 367
King I. R., 1966, AJ, 71, 64
Kontizas M., Hatzidimitriou D., Bellas-Velidis I., Gouliermis D., Kontizas E., Cannon R. D., 1998, A&A, 336, 503
Kroupa P., 2000, in Deiters S., Fuchs B., Just A., Spurzem R., Wielen R., eds, ASP Conf. Ser. Vol. 228, Dynamics of Star Clusters and the Milky Way. Astron. Soc. Pac., San Francisco, in press (astro-ph/0011328)
Kroupa P., Tout C. A., 1997, MNRAS, 287, 402
Kroupa P., Tout C. A., Gilmore G. F., 1990, MNRAS, 244, 76
Kroupa P., Tout C. A., Gilmore G. F., 1993, MNRAS, 262, 545 (KTG93)
Lada C. J., 1991, in Lada C. J., Kylafis N. D., eds, The Physics of Star Formation and Early Stellar Evolution. Kluwer, Dordrecht, p. 329
Larson R. B., 1991, in Falgarone E., Boulanger F., Duvert G., eds, Proc. IAU Symp. 147, Fragmentation of Molecular Clouds and Star Formation. Kluwer, Dordrecht, p. 261
Leggett S. K., Allard F., Berriman G., Dahn C. C., Hauschildt P. H., 1996, ApJS, 104, 117
Lejeune T., Cuisinier F., Buser R., 1998, A&AS, 130, 65
Lightman A. P., Shapiro S. L., 1978, Rev. Mod. Phys., 50, 437
Malumuth E. M., Heap S. R., 1994, AJ, 107, 1054
McClure R. D. et al., 1986, ApJ, 307, L49
Meliani M. T., Barbuy B., Richtler T., 1994, A&A, 290, 753
Meylan G., 1987, A&A, 184, 144
Nemec J. M., Harris H. C., 1987, ApJ, 316, 172
Oliva E., Origlia L., 1998, A&A, 332, 46
Piotto G., Cool A. M., King I. R., 1997, AJ, 113, 1345
Popper D. M., 1980, ARA&A, 18, 115
Pryor C., Smith G. H., McClure R. D., 1986, AJ, 92, 1358
Richer H. B., Fahlman G. G., 1987, ApJ, 316, 189
Richer H. B., Fahlman G. G., 1989, ApJ, 339, 178
Rubenstein E. P., Bailyn C. D., 1999, ApJ, 513, L33

Ryan S. G., Norris J. E., 1991, AJ, 101, 1865
Salpeter E. E., 1955, ApJ, 121, 161
Santiago B. X., Beaulieu S., Johnson R., Gilmore G. F., 2001, A&A, 369, 74
Santos J. F. C., Jr, Bica E., Claría J. J., Piatti A. E., Girardi L. A., Dottori H., 1995, MNRAS, 276, 1155
Saviane I., Piotto G., Fagotto F., Zaggia S., Capaccioli M., Aparicio A., 1998, A&A, 333, 479
Scalo J. M., 1986, Fundam. Cosmic Phys., 11, 1
Shu F. H., Adams F. C., Lizano S., 1987, ARA&A, 25, 23
Sosin C., 1997, AJ, 114, 1517
Sosin C., King I. R., 1997, AJ, 113, 1328
Spitzer L., 1969, ApJ, 158, L139
Spitzer L., Hart M. H., 1971, ApJ, 164, 399
Spitzer L., Shull J. M., 1975, ApJ, 201, 773
Tout C. A., Pols O. R., Eggleton P. P., Han Z., 1996, MNRAS, 281, 257 (TPEH96)
van Bever J., Vanbeveren D., 1997, A&A, 322, 116
Vesperini E., Heggie D. C., 1997, MNRAS, 289, 898
Will J.-M., Bomans D. J., de Boer K. S., 1995, A&A, 295, 54

This paper has been typeset from a TEX/LATEX file prepared by the author.